

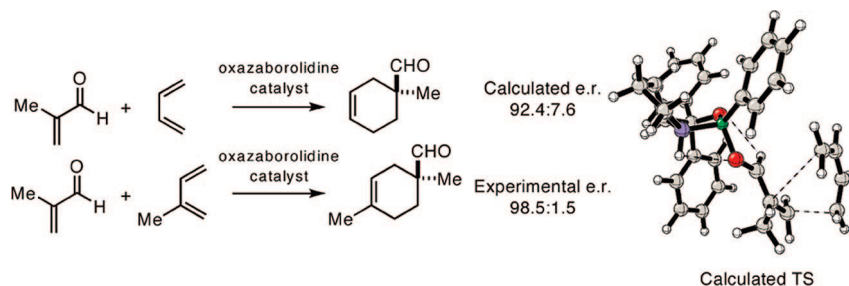
Computational Evaluation of Enantioselective Diels–Alder Reactions Mediated by Corey’s Cationic Oxazaborolidine Catalysts

Michael N. Paddon-Row,^{*,†} Christopher D. Anderson,[‡] and K. N. Houk^{*,‡}

School of Chemistry, University of New South Wales, Sydney 2052, Australia, and Department of Chemistry and Biochemistry, University of California, Los Angeles, California 90095-1569

m.paddonrow@unsw.edu.au; houk@chem.ucla.edu

Received October 15, 2008



The cationic oxazaborolidine-catalyzed Diels–Alder reactions of butadiene and a series of five dienophiles have been studied using density functional theory (B3LYP/6-31G(d)). In each case, the computational results successfully reproduce the experimentally observed sense of stereoselection and enantiomeric ratio. The computed structures of the lowest energy Lewis acid–carbonyl complexes and Lewis acid–transition state complexes are closely related to the models for stereoselection proposed by Corey and co-workers.

Introduction

Diels–Alder (DA) reactions are among the most powerful synthetic methods available to chemists.¹ Given the broad synthetic utility of this transformation, procedures for controlling the absolute configuration of the cycloadducts, either by the use of chiral auxiliaries or chiral catalysts, have been eagerly sought.² To date, several asymmetric variants of the DA reaction have been developed that produce cycloaddition products in high yield (>90%) and high stereoselectivity (>90% ee), while proceeding with predictable stereochemical outcomes. Corey and co-workers have developed one of the most elegant methods utilizing an amino-acid-derived oxazaborolidinium ion catalyst (Figure 1).^{2a,3}

The Corey asymmetric DA methodology utilizes a chiral, cationic oxazaborolidine catalyst **3** derived from proline (Figure

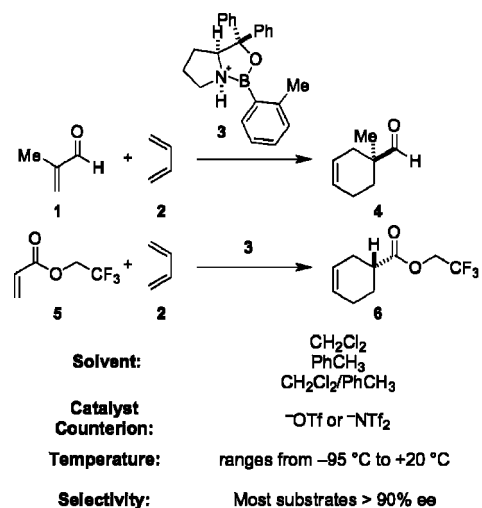


FIGURE 1. Overview of Corey’s asymmetric Diels–Alder reaction.

1). A wide variety of α,β -unsaturated carbonyl compounds (aldehydes, ketones, esters, quinones, and carboxylic acids) are efficient substrates in this reaction, being readily converted to enantioenriched cyclohexenes of >90% enantiomeric excess in the presence of ≤ 20 mol % of catalyst **3**.³ In addition to the

[†] University of New South Wales.

[‡] University of California, Los Angeles.

(1) Nicolaou, K. C.; Snyder, S. A.; Montagnon, T.; Vassilikogiannakis, G. *Angew. Chem., Int. Ed.* **2002**, *41*, 1668–1698.

(2) (a) Corey, E. J. *Angew. Chem., Int. Ed.* **2002**, *41*, 1650–1667. (b) Kagan, H. B.; Riant, O. *Chem. Rev.* **1992**, *92*, 1007–1019.

(3) (a) Ryu, D. H.; Lee, T. W.; Corey, E. J. *J. Am. Chem. Soc.* **2002**, *124*, 9992–9993. (b) Corey, E. J.; Shibata, T.; Lee, T. W. *J. Am. Chem. Soc.* **2002**, *124*, 3808–3809. (c) Ryu, D. H.; Corey, E. J. *J. Am. Chem. Soc.* **2003**, *125*, 6388–6390. (d) Ryu, D. H.; Zhou, G.; Corey, E. J. *J. Am. Chem. Soc.* **2004**, *126*, 4800–4802.

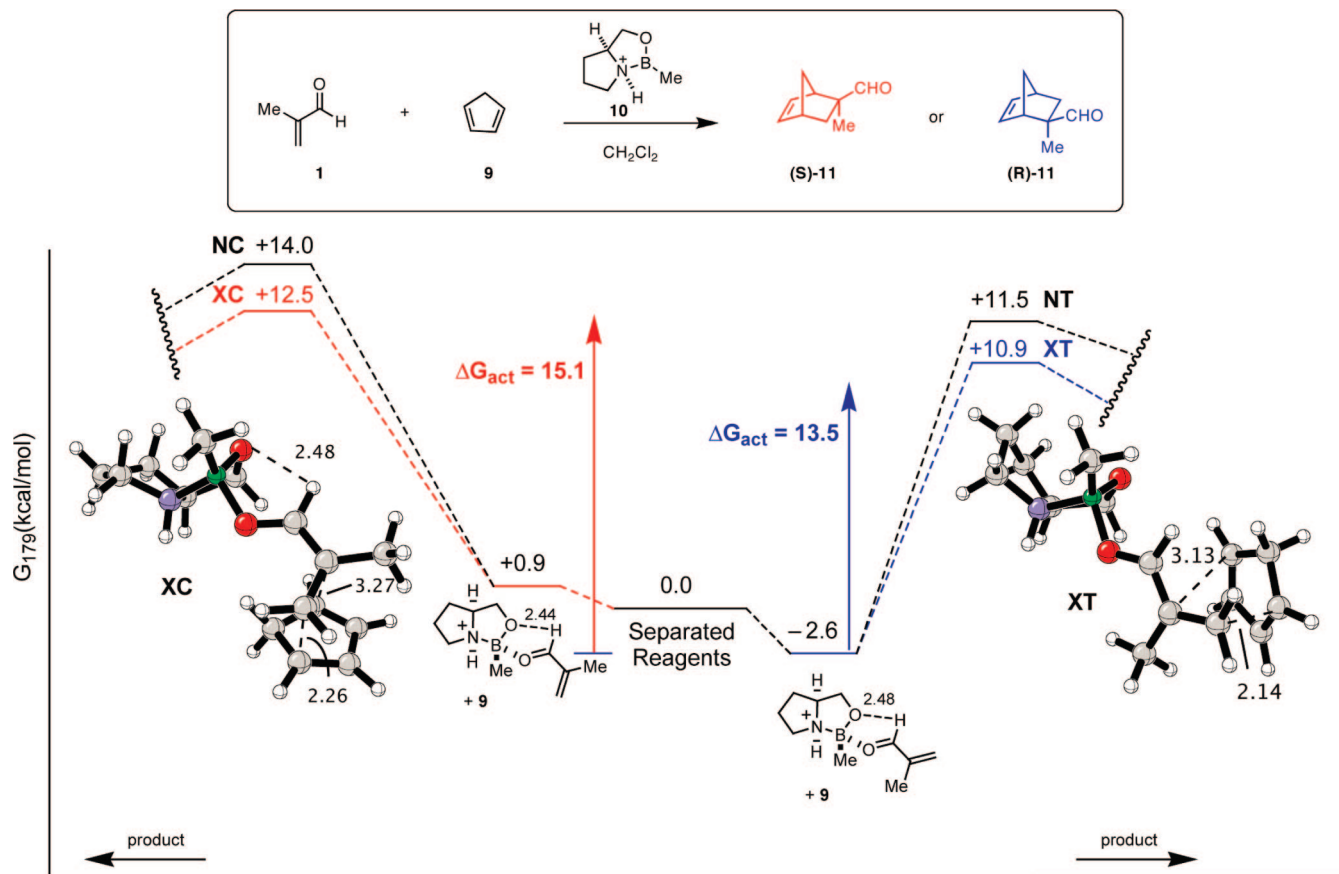
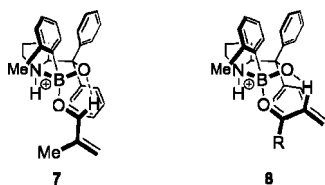


FIGURE 2. Summary of the computational results of Pi and Li.⁶ Geometries and relative energies were determined at the PCM-B3LYP/6-31G(d,p) level. The experimentally observed major enantiomer is (*S*)-**11**, which is predicted to arise from the **XC** TS, whereas the minor enantiomer (*R*)-**11** arises from the **XT** TS.

generality of this method, the stereochemical outcome of this process can be predicted using Corey's models. For aldehydes, coordination of the carbonyl oxygen with the boron of the catalyst and a C–H···O interaction^{4,5} between the catalyst oxygen and the aldehyde C–H form a complex where the *si* face of the dienophile is shielded by the pseudoaxial phenyl ring of the catalyst, as illustrated by model **7**. In the case of other α,β -unsaturated carbonyl compounds (ketones, esters, quinones, and carboxylic acids), Corey proposed model **8**. In these cases, the primary interaction remains the carbonyl oxygen–boron interaction; however, the secondary interaction is now between the α -C–H and the catalyst oxygen, which provides both a rigidified complex and a means of biasing the dienophile geometry.⁴ Two significant features of models **7** and **8** are (1) the adoption of the *s-trans* conformation of the α,β -unsaturated carbonyl dienophile and (2) the fact that the diene always attacks the dienophile from the less hindered “nitrogen” side of the complex, rather than from the “C5-diphenyl” side. In all of the examples of intermolecular DA reactions utilizing catalyst **3** published to date, these models correctly predict the outcome of the reactions.



Recently, Pi and Li reported the results of a DFT study of the mechanism of the oxazaborolidinium ion-catalyzed DA reaction between 2-methyl acrolein (**1**) and cyclopentadiene (**9**) (Figure 2).⁶ Using a simplified model catalyst **10** and evaluating four possible transition structures (**NC**, **XC**, **NT**, **XT**, where N represents *endo* cycloaddition, X represents *exo* cycloaddition, C represents *s-cis* conformation of the dienophile, and T represents *s-trans* conformation of the dienophile), Pi and Li determined that the *exo/s-cis* or **XC** mode is energetically the most favorable and leads to formation of (*S*)-**11**, the experimentally observed major enantiomer of the *exo* adduct. The Pi–Li study raises two important issues. First, the predicted favored **XC** TS, where the diene approaches the dienophile in the *s-cis* conformation from the “C5” side, is at odds with the successful Corey TS model, where the diene approaches the dienophile in the *s-trans* conformation from the “nitrogen” side. Second, although one can find many examples of *exo* Diels–Alder reactions between cyclopentadiene and 2-substituted acrolein derivatives, there is little experimental evidence that suggests that 2-substituted acrolein derivatives will undergo cycloaddition reactions via the *s-cis* conformation preferentially.

This observation led us to more closely evaluate the report by the Nanjing group. Upon closer inspection, it became clear

(4) (a) Corey, E. J.; Rohde, J. J.; Fischer, A.; Azimioara, M. D. *Tetrahedron Lett.* **1996**, *38*, 33–36. (b) Corey, E. J.; Rohde, J. J. *Tetrahedron Lett.* **1997**, *38*, 37–40. (c) Corey, E. J.; Barnes-Seeman, D.; Lee, T. W. *Tetrahedron Lett.* **1997**, *38*, 4351–4354.

(5) Wong, M. W. *J. Org. Chem.* **2005**, *70*, 5487–5493.

(6) Pi, Z.; Li, S. *J. Phys. Chem. A* **2006**, *110*, 9225–9230.

that their conclusions rested on the assumption that complexes formed between the Lewis acid and carbonyl compounds undergo reaction faster than these complexes dissociate. If this were the case, the stereoselectivity of the reaction would be determined by the step in which the Lewis acid–carbonyl complex is formed. However, one need only look at the computational results of Pi and Li to see that in this case the free energy of complexation is much smaller than the free energy of activation for this Diels–Alder reaction (2.51 vs 12.51 kcal/mol).⁷ Thus, the Winstein–Holness equation⁸ can be used to describe the reaction kinetics, and the product distribution can be interpreted using the Curtin–Hammett principle.^{9,10} That is, the relative transition structure free energies correspond to the enantioselectivity of this reaction. The **XT** (*exols-trans*) mode of cycloaddition should be most favorable. Unfortunately, the **XT** transition state leads to the formation of aldehyde (**R**)-**11**, which is not consistent with experiment (Figure 2). Thus, the Pi and Li computations fail to correlate with experimental observations. This failure might be due to their use of the highly simplified oxazaborolidinium cation catalyst **10** in which the crucial B-phenyl and C5-diphenyl substituents were replaced with a B-methyl group and two hydrogen atoms at C5. The significantly smaller steric influence of the C5-methylene in the Pi and Li catalyst **10**, compared to the C5-diphenyl group in Corey's catalyst **3**, would explain why the diene appears to prefer the “anti-Corey” approach from the “C5” side in Pi and Li's system.

Given the shortcomings of the previous investigation, an exhaustive computational effort was warranted to clarify the mechanistic origin of enantioselectivity of oxazaborolidinium-catalyzed DA reactions and to verify the correctness of Corey's pretransition state models for predicting, qualitatively, the observed enantioselectivities in a variety of DA reactions involving various dienophiles. Recently, Paddon-Row et al. reported a computational study of oxazaborolidinium-catalyzed intramolecular DA reactions that showed, among other things, that the Curtin–Hammett approximation holds in such catalyzed IMDA reactions and that predicted enantioselectivities, derived solely from differences in the transition structure free energies, were in good accord with the experimental enantioselectivities.¹¹ This computational study extends the scope of that earlier work by investigating, using density functional theory (B3LYP/6-31G(d)), oxazaborolidinium-catalyzed intermolecular DA reactions of 1,3-butadiene with several different dienophiles, namely, methacrolein (**1**), acrolein (**12**), methyl acrylate (**13**), dimethyl fumarate (**14**), and 2-methylbenzoquinone (**15**) (Figure 3).

Computational Methods

Gas-phase reactants, reactant complexes, and transition structures (TSs) for oxazaborolidinium cation-catalyzed Diels–Alder (DA) reactions were optimized using the B3LYP functional¹² and the 6-31G(d)¹³ basis set. Despite its oft-cited shortcomings, the B3LYP/6-31G(d) level of theory is known to give an excellent account of DA reactivity and selectivity.^{14,15} Harmonic vibrational frequencies (at the same level of theory) were employed to characterize the

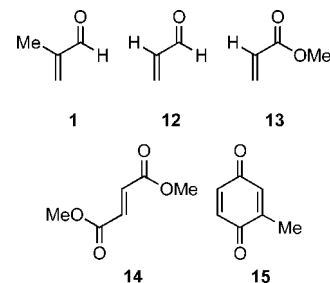


FIGURE 3. Dienophiles evaluated in the current investigation.

reactants and TSs as zero-order and first-order (i.e., one negative Hessian eigenvalue) saddle points, respectively. The unscaled vibrational frequencies were also used to calculate the enthalpies and free energies of the reactants and TSs at 298.15 K and 1 bar pressure. Product distributions and enantioselectivities at 298.15 K were calculated using the rate expression derived from standard transition state theory.^{16,17} Nonspecific solvent effects on the enantioselectivities for selected DA reaction were studied within the context of self-consistent reaction field theory using the polarizable continuum model (PCM)¹⁸ and dichloromethane as solvent ($\epsilon = 8.93$). The cavity for each PCM calculation was constructed using the united atom topological model (UA0), together with the solvent accessible surface procedure.¹⁹ As in the gas-phase calculations, harmonic vibrational frequencies were calculated for the PCM optimized geometries. In a number of cases, intrinsic reaction coordinate calculations were carried out on the lowest energy TSs in order to confirm that the TSs did, indeed, lead to the formation of oxazaborolidinium cation complexes of the DA products.²⁰ Optimized geometries (in Cartesian coordinate form) and their energies, enthalpies, and free energies for the four most stable TSs for each catalyzed DA reaction are provided in

(12) (a) Lee, C.; Yang, W.; Parr, R. G. *Phys. Rev. B* **1988**, *37*, 785–789. (b) Becke, A. D. *J. Chem. Phys.* **1993**, *98*, 5648–5652. For reviews of density functional methods see: (c) Ziegler, T. *Chem. Rev.* **1991**, *91*, 651–667. (d) *Density Functional Methods in Chemistry*; Labanowski, J. K., Andzelm, J. W., Eds.; Springer-Verlag: New York, 1991. (e) Parr, R. G.; Yang, W. *Density-Functional Theory of Atoms and Molecules*; Oxford University Press: New York, 1989. (f) Koch, W.; Holthausen, M. C. *A Chemist's Guide to Density Functional Theory*; Wiley-VCH: Weinheim, 2000.

(13) (a) Hehre, W. J.; Radom, L.; Schleyer, P. v. R.; Pople, J. A. *Ab Initio Molecular Orbital Theory*; John Wiley & Sons, Inc.: New York, 1986. (b) *The Encyclopedia of Computational Chemistry*; Schleyer, P. v. R., Allinger, N. L., Clark, T., Gasteiger, J., Kollman, P. A., Schaefer, H. F., III, Schreiner, P. R., Eds.; John Wiley & Sons, Ltd.: Chichester, 1998.

(14) (a) Wiest, O. G.; Montiel, D. C.; Houk, K. N. *J. Phys. Chem. A* **1997**, *101*, 8378–8388. (b) Kong, S.; Evanseck, J. D. *J. Am. Chem. Soc.* **2000**, *122*, 10418–10427. (c) Paddon-Row, M. N.; Moran, D.; Jones, G. A.; Sherburn, M. S. *J. Org. Chem.* **2005**, *70*, 10841–10853. (d) Cayzer, T. N.; Paddon-Row, M. N.; Moran, D.; Payne, A. D.; Sherburn, M. S.; Turner, P. *J. Org. Chem.* **2005**, *70*, 5561–5570.

(15) For examples of calculations considering boron Lewis acid catalyzed DA reactions, see: (a) Alves, C. N.; Carneiro, A. S.; Andrés, J.; Domingo, L. R. *Tetrahedron* **2006**, *62*, 5502–5509. (b) Salvatella, L.; Ruiz-López, M. F. *J. Am. Chem. Soc.* **1999**, *121*, 10772–10780. For an example of calculations considering organic cation-catalyzed DA reactions, see: (c) Sun, H.; Zhang, D. J.; Ma, C.; Liu, C. B. *Int. J. Quantum Chem.* **2007**, *107*, 1875–1885.

(16) Moore, J. W.; Pearson, R. G. *Kinetics and Mechanism*, 3rd ed.; John Wiley & Sons Inc.: New York, 1981; Chapter 7.

(17) Experimental selectivity was obtained from reactions performed at a variety of temperatures ranging from –95 to –20 °C. See ref 3.

(18) (a) Miertus, S.; Scrocco, E.; Tomasi, J. *Chem. Phys.* **1981**, *55*, 117–129. (b) Miertus, S.; Tomasi, J. *Chem. Phys.* **1982**, *65*, 239–245. (c) Cossi, M.; Barone, V.; Cammi, R.; Tomasi, J. *Chem. Phys. Lett.* **1996**, *255*, 327–335. (d) Cammi, R.; Mennucci, B.; Tomasi, J. *J. Phys. Chem. A* **2000**, *104*, 5631–5637. (e) Cossi, M.; Scalmani, G.; Rega, N.; Barone, V. *J. Chem. Phys.* **2002**, *117*, 43–54.

(19) The solvent accessible molecular surface (using the solvent excluding surface in the PCM geometry optimizations) invariably led to failure in convergence, notwithstanding calculating the Hessian matrix at each optimization cycle.

(20) (a) Gonzalez, C.; Schlegel, H. B. *J. Chem. Phys.* **1989**, *90*, 2154–2161. (b) Gonzalez, C.; Schlegel, H. B. *J. Phys. Chem.* **1990**, *94*, 5523–5527.

(7) In addition, rapid exchange between Lewis acids and Lewis bases has been observed experimentally by NMR techniques. See: Farcașiu, D.; Stan, M. *J. Chem. Soc., Perkin Trans. 2* **1998**, 1219–1222.

(8) Winstein, S.; Holness, N. J. *J. Am. Chem. Soc.* **1955**, *77*, 5562–5578.

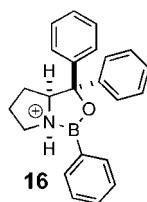
(9) Pollak, P. I.; Curtin, D. Y. *J. Am. Chem. Soc.* **1950**, *72*, 961–965.

(10) For a review, see: Seeman, J. I. *Chem. Rev.* **1983**, *83*, 83–134.

(11) Paddon-Row, M. N.; Kwan, L. H. C.; Sherburn, M. S. *Angew. Chem., Int. Ed.* **2008**, *47*, 7013–7017.

Supporting Information. The Gaussian 03 suite of programs was used for all calculations.²¹

To best mimic the Corey DA reaction, we chose a model oxazaborolidinium catalyst **16** that only differs from the commonly used experimental catalyst **3** by the removal of the methyl group from the *o*-tolyl substituent attached to boron. Indeed, **16** was employed in earlier studies by Corey but was abandoned in favor of **3** because the latter catalyst gave consistently higher enantioselectivities.^{3b} This simplification reduced the computational cost of this study by a factor of 2, as it removed the need to consider the two rotational isomers about the B–Ar bond. Corey demonstrated experimentally that this catalyst modification led to a small reduction in enantioselectivity (95:5 ratio favoring *S* with the B-*o*-tolyl catalyst **3** to 87.5:12.5 ratio favoring *S* with the B-Ph catalyst **16**).^{3b} As such, model catalyst **16** was deemed suitable for this investigation.



We have focused our attention on the *endo* cycloaddition of butadiene to the various dienophiles, because Corey and co-workers only observe the products of *endo* addition for comparable reactions. Indeed, previous computational studies on the Lewis acid catalyzed butadiene-acrolein DA reaction predict strong *endo* selectivity.²² We did, however, investigate the *endo* versus *exo* selectivity in the oxazaborolidinium cation-catalyzed DA reaction between butadiene and methyl acrylate and found that *endo* attack is favored over *exo* attack by 0.5 kcal/mol (enthalpy) and 0.5 kcal/mol (free energy) at 298 K.

Gas-phase calculations were first carried out for each DA reaction in order to verify that the B3LYP/6-31G(d) theoretical model was able to find that the lowest energy TS corresponds to the experimentally favored enantiomer without introducing too much bias resulting from restrictive choice of candidate TSs for study. To this end, we systematically evaluated possible transition structures for each reaction. We considered for each system (1) the approach of the diene to each of the enantiotopic faces of the dienophile, (2) the possible modes of coordination of the catalyst to dienophile (e.g., *a* and *b*, Figure 4), (3) the possible modes of coordination of the dienophile to the catalyst, both to the sterically less congested *exo* face of the oxazaborolidinium cation and to the more congested *endo* face of the catalyst (Figure 4), and (4) the possible conformations of the dienophile (e.g., *s-cis*, *s-trans*, etc.) For DA reactions involving acrolein, methacrolein, and methyl acrylate, all 16 TSs and eight reactant complexes were calculated for each system (as shown in Figure 4, there are two complexation sites and two conformations, *cisoid* and *transoid*, for the carbonyl group with respect to the dienophile double bond). For the DA reaction involving methyl acrylate, an additional 16 TSs, for a combined total of 32 TSs, in which the OMe group adopts the less favorable²³ *anti* conformation with respect to the carbonyl group were calculated (Figure 4). For 2-methylbenzoquinone dienophiles, both complexation at the four different oxygen lone pair site, *a–d*, and attack of butadiene at the two different double bonds were considered (Figure 4). In this way 32 TSs and eight unique 2-methylbenzoquinone–

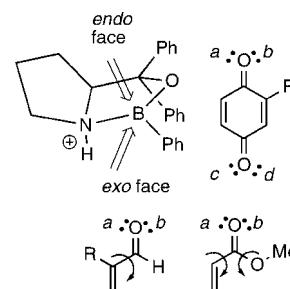


FIGURE 4. Complexation sites at the oxazaborolidinium cation (*endo* face or *exo* face) and at the oxygen atom of various dienophiles (*a*, *b*). In addition, the carbonyl group of acrolein and methacrolein (lower left; R = H and Me, respectively) may adopt either the *cisoid* (not shown) or *transoid* (shown) conformation with respect to the dienophile double bond (the *cisoid*–*transoid* interconversion is depicted by a curved arrow). In addition, the OMe group in methyl acrylate (lower right) may adopt either the *syn* (shown) or *anti* (not shown) conformation with respect to the carbonyl group.

TABLE 1. Gibbs Free Energies of Formation ($\Delta G_{\text{complex}}$) of the Most Stable Complexes of Catalyst **16** and Substrate and DA Gibbs Free Energies of Activation (ΔG_{act}) Relative to These Complexes^a

substrate	gas phase		dichloromethane solvent ^b	
	$\Delta G_{\text{complex}}$	ΔG_{act}	$\Delta G_{\text{complex}}$	ΔG_{act}
1	–3.3	+18.5	–1.3	+18.1
13	–1.3	+24.2	+0.2	+24.4
15	–1.3	+21.4	+0.4	+21.4

^a Energies calculated at the B3LYP/6-31G(d) level of theory and reported in kcal/mol. ^b Nonspecific solvent effect by using the polarizable continuum model.

oxazaborolidinium cation complexes are possible and were calculated for this system. Finally, a restricted set of 16 TSs and eight reactant complexes were calculated for the DA reaction involving dimethyl fumarate. For this system, complexation at site *b* was ignored on the grounds that this mode of complexation in the methyl acrylate system is at least 5 kcal/mol less favorable than complexation at site *a*. In the TSs and reactant complexes for dimethyl fumarate, the uncomplexed ester group of dimethyl fumarate was allowed to adopt both *cisoid* and *transoid* conformations. Overall, more than 100 transition structures (TSs) were located in the course of this investigation.

Results and Discussion

The conclusions presented herein are largely based upon gas-phase geometries. The rationale for neglecting nonspecific solvent effects is based upon a comparison of gas phase and PCM calculations for methacrolein (**1**), methyl acrylate (**13**) and 2-methylbenzoquinone (**15**) with butadiene catalyzed by oxazaborolidinium ion **16**. In each case, the two lowest energy transition structures (at minimum) had the same conformation both in the gas phase and in the PCM calculation. For each of these three systems, the two lowest TSs represent the reaction pathway for >90% of the reactants, based on Boltzmann population calculations using activation free energy.¹⁶ In addition, the values of ΔG_{act} in the gas phase are within 0.5 kcal/mol of the values of ΔG_{act} in dichloromethane. Given the small differences between the PCM and gas-phase calculations, the discussion presented herein will focus exclusively on the gas-phase results.

The data presented in Table 1 also clearly show that, for each system, the numerical value of the free energy of complexation is considerably smaller than the corresponding free energy of

(21) Frisch, M. J. et al. *Gaussian 03, Revision D.01*; Gaussian, Inc.: Pittsburgh, PA, 2003.

(22) (a) Birney, D. M.; Houk, K. N. *J. Am. Chem. Soc.* **1990**, *112*, 4127–4133. (b) García, J. I.; Martínez-Merino, V.; Mayoral, J. A.; Salvatella, L. *J. Am. Chem. Soc.* **1998**, *120*, 2415–2420. (c) García, J. I.; Mayoral, J. A.; Salvatella, L. *Tetrahedron* **1997**, *53*, 6057–6064.

(23) Wang, X.; Houk, K. N. *J. Am. Chem. Soc.* **1988**, *110*, 1870–1872.

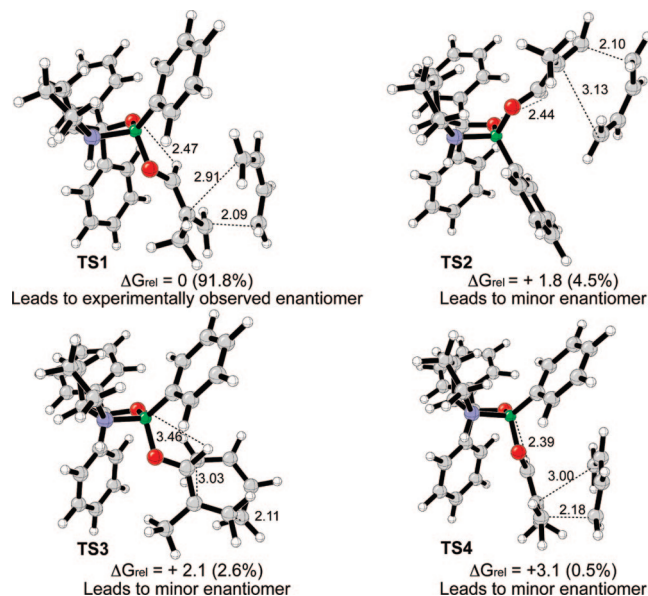


FIGURE 5. Four lowest energy transition structures for DA reaction of methacrolein and butadiene. Distances are shown in angstroms, relative free energies in kcal/mol, and percentages of each TS in the gas phase are listed in parentheses.

activation for the cycloaddition reaction. Assuming that complex formation is essentially barrierless, we conclude that complex formation is rapidly reversible on the DA reaction time scale. In fact, it has been shown that the association of an α,β -enal and a cognate oxazaborolidine catalyst is rapidly reversible on the NMR time scale.²⁴ Consequently, the enantioselectivities of the DA reactions studied herein are determined solely by the relative free energies of competing TSs.

Acrolein and Methacrolein. As mentioned above, an exhaustive transition structure search was performed for the reaction between methacrolein and 1,3-butadiene, considering 16 different transition structure conformations. The four lowest energy geometries are illustrated in Figure 5. Bond formation in each of these structures is asynchronous, as would be expected on the basis of calculations of less complex Lewis acid catalyzed Diels–Alder reactions.²² The low energy TS conformation (TS1) for this reaction is remarkably similar to the transition state model proposed by Corey and co-workers with the carbonyl group coordinated to the *exo* (convex) face of the oxazaborolidinium ion catalyst and the aldehyde C–H positioned proximal to the oxygen atom of the catalyst, allowing for a C–H \cdots O interaction (Figure 5).⁴ The diene approaches the dienophile from the sterically accessible side (*re* face addition) leading to the experimentally observed enantiomer. Looking at the next higher energy TS (TS2) demonstrates that 2.6% of product arises from a TS where the dienophile is coordinated to the *endo* (concave) face of the catalyst, which is an unexpected result. In the next higher energy TS (TS3), the dienophile has rotated 59° such that the aldehyde C–O forms a 38° dihedral angle with the B–Ar bond and the C–H \cdots O interaction is significantly reduced. This rotation allows for approach of the diene from the *si* face of the dienophile and leads to formation of the minor enantiomer. The final illustrated TS (TS4) shares much in common with TS1 with the distinguishing characteristic being the conformation of the dienophile, which is *s-cis* in this case.

In sum, the four lowest energy TSs represent the pathway to product formation for 99.4% of the reactants. The remaining 12 TSs that were calculated represent the remaining modes leading to product.

The calculated free energies of activation for all 16 TSs were used to calculate the selectivity for methacrolein–butadiene reaction. On the basis of the calculated TS energies, the selectivity for this process is predicted to be 92.4:7.6 favoring the (*S*)-enantiomer of cyclohexene carboxaldehyde **17** (Table 2, entry 1). The most similar experimental example differs by a single methyl group and produces the product as a 98.5:1.5 mixture of enantiomers favoring the (*S*)-enantiomer of aldehyde **18** (Table 2, entry 1). Thus DFT calculations were able to successfully reproduce the experimental selectivity for the 2-methylacrolein DA reaction within 3 percentage points.

In the case of acrolein, Corey’s model for selectivity was reinforced by this investigation. The calculated and experimental values for selectivity (Table 2, entry 2) are in excellent agreement (within 0.5 percentage points). The lowest energy transition structure TS5 mirrors Corey’s model for selectivity with both the B \cdots O interaction and a C–H \cdots O interaction, and a *s-trans* geometry of the coordinated acrolein (Figure 6). The second most stable TS (1.5 kcal/mol higher in energy than TS5) produces the minor enantiomer and involves coordination to the *endo* (concave) face of the catalyst (TS6). The third most stable TS (1.7 kcal/mol less stable than TS5) is TS7. It contains a coordinated acrolein molecule in a *s-cis* configuration and leads to the generation of the minor enantiomer. The fourth most favorable TS, which also leads to the minor enantiomer, lacks a C–H \cdots O interaction and as a result of the rotation of the acrolein molecule allows the diene to approach from the opposite enantiotopic face of the dienophile (analogous to TS3, Figure 5). This TS is calculated to be only 1.9 kcal/mol higher in energy than TS5.

These results contrast to those of García and co-workers, who studied the BF₃-catalyzed DA reaction of acrolein and 1,3-butadiene using B3LYP/6-31G(d).^{22b} In their investigation, the lowest energy TS was found to be composed of an acrolein molecule that adopted a *s-cis* orientation with an *endo* approach of the dienophile. The TS with a *s-trans* oriented acrolein molecule and the *endo* approach of the dienophile was 2.5 kcal/mol higher in energy. In systems involving catalyst **16**, the *s-trans* conformation of the coordinated α,β -unsaturated aldehyde is preferred as a result of the steric bias introduced by the B-phenyl substituent. As can be seen in Figure 6, the approach of 1,3-butadiene to the *s-cis* dienophile in TS7 is severely limited by the presence of this substituent, whereas in TS5 the approach of the dienophile to the *s-trans* dienophile is unimpeded.

Acrylates and Fumarates. Corey also demonstrated that the Diels–Alder reactions of acrylates catalyzed by oxazaborolidinium **3** (Table 2, entry 3) are highly selective, and again DFT calculations are in agreement with this observation. In this instance, theory predicts the enantiomer ratio within 1 percentage point of the experimental value. The low energy TS (TS8) contains all the features of the Corey model **8**, which include the B \cdots O interaction on the *exo* face of the catalyst, the C–H \cdots O interaction, the *s-trans* orientation of the dienophile, and the *endo* approach of the diene (Figure 7). In addition, coordination of the carbonyl occurs via the lone pair *syn* with the double bond (site *a*, Figure 4), which is also in accord with the Corey model. As was true in the DA reactions described above, one of the low energy TSs for the acrylate DA reaction involves

(24) Corey, E. J.; Loh, T.-P.; Roper, T. D.; Azimioara, M. D.; Noe, M. C. *J. Am. Chem. Soc.* **1992**, *114*, 8290–8292. Also see ref 7.

TABLE 2. Computed Reaction Selectivity Compared to Experimental Selectivity

Entry	Computed Reactions	Enantiomeric Ratio ^a (calculated)	Similar Experimental Examples	Enantiomeric Ratio ^a (experimental)
1		92.4:7.6		98.5:1.5 Ref. 3b
2		84:16		84.5:15.5 Ref. 3a
3		96.8:3.2		97.5:2.5 Ref. 3c
4		94.7:5.3		96.5:3.5 Ref. 3c
5		68.6:31.4 ^b (64:36) ^c		95.5:4.5 Ref. 3d

^a Major enantiomer illustrated. ^b Enantiomer ratio considering only TS geometries with catalyst coordination to the C4 carbonyl. ^c Enantiomer ratio considering TS geometries with catalyst coordination to both carbonyl groups. ^d Enantiomer ratio considering only TS geometries with catalyst coordination to the C1 carbonyl.

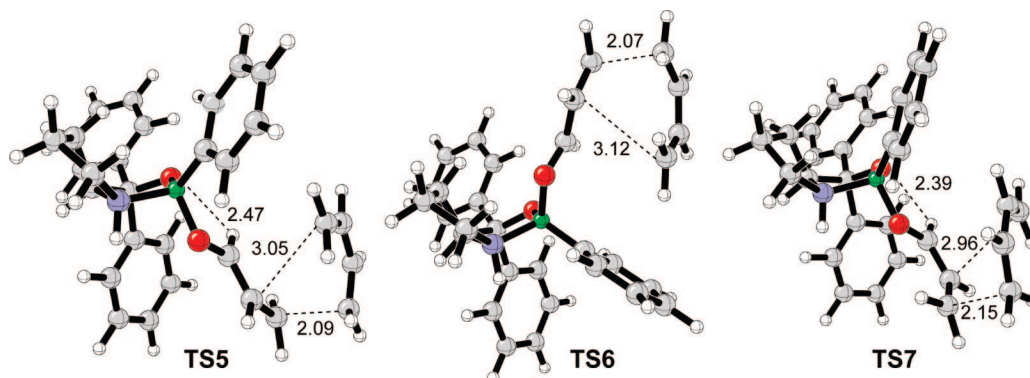


FIGURE 6. Low energy TS for the DA reaction of acrolein and 1,3-butadiene (TS5), the lowest energy TS with acrolein complexed to the *endo* face of the oxazaborolidinium catalyst (TS6), and the lowest energy TS with a *s-cis* acrolein molecule (TS7). Distances are listed in angstroms.

coordination to the concave face of the oxazaborolidinium ion catalyst. In the case of methyl acrylate, the second most favorable TS (2.2 kcal/mol less stable than TS8) has such a coordination mode, which leads to the formation of the minor enantiomer.

The DA reactions of fumarates catalyzed by chiral Lewis acid **3** are also largely selective for a single enantiomer (Table 2, entry 4), and DFT calculations of dimethyl fumarate DA reactions catalyzed by oxazaborolidinium ion **16** also predict the selectivity within 2 percentage points of the experimentally observed value. Again, Corey's model **8** predicts all of the key features in the major transition structure TS9, which are analogous to those mentioned in the methyl acrylate DA case. As in the other examples, one of the contributing transition structures leading to the minor enantiomer involves coordination of the dienophile to the concave face of catalyst **16**. In the case

of dimethyl fumarate, the lowest energy *endo*-coordinated TS is 2.1 kcal/mol less stable than TS9.

2-Methylbenzoquinone. The final substrate that was considered in this study, 2-methylbenzoquinone, lends some further support to the Corey model. However, in this case agreement between the experimental and computational results is less clear (Table 2, entry 5). In entry 5 of Table 2, the computational prediction for selectivity is 27 percentage points less than the experimental value (68.6:31.4 vs 95.5:4.5). The three lowest energy TSs, which represent the pathway for the formation of 85.5% of the product, are shown in Figure 8. The lowest energy TS (TS10) corresponds to the Corey model with coordination of the most basic lone pair of electrons to the catalyst (site *c*, Figure 4) and the α -C–H engaged in an interaction with the catalyst oxygen atom, and the cycloaddition occurs with the double bond that

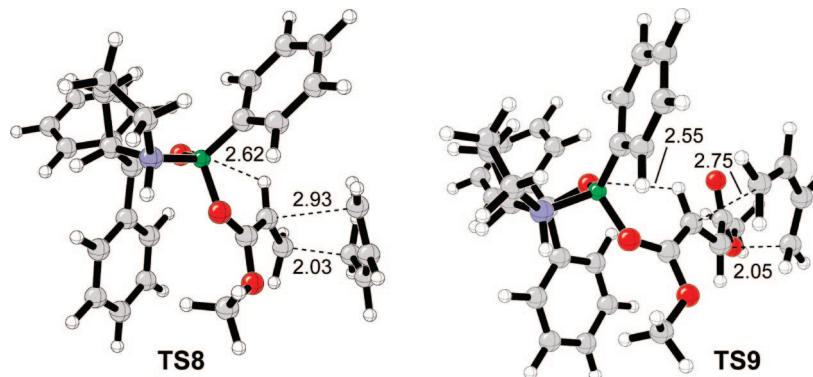


FIGURE 7. Lowest energy TSs for the methyl acrylate-1,3-butadiene DA reaction (**TS8**) and dimethyl fumarate-1,3-butadiene DA reaction (**TS9**). Distances are listed in angstroms.

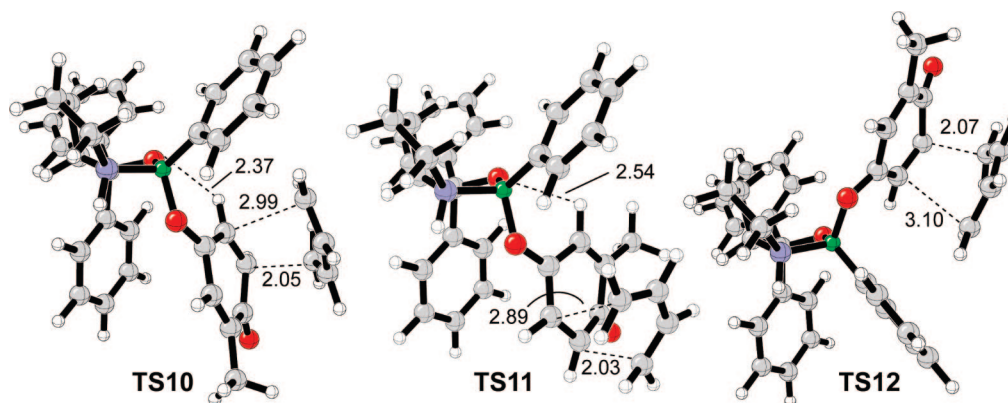


FIGURE 8. Low energy TS for the DA reaction of 2-methylbenzoquinone and 1,3-butadiene (**TS10**), lowest energy TS for cycloaddition with double bond *anti* to the coordination site (**TS11**) and the lowest energy TS for the same reaction with 2-methylbenzoquinone complexed to the *endo* face of the oxazaborolidinium catalyst (**TS12**). Distances are listed in angstroms.

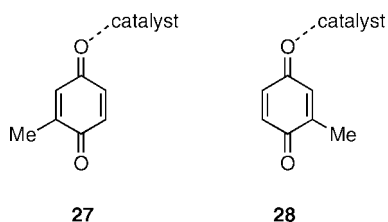


FIGURE 9. Schematic low energy coordination modes for catalyst **16** with 2-methylbenzoquinone. Complex **27** is related to **TS10**, where the catalyst is coordinated *anti* to the substituted double bond, and complex **28** is related to **TS11**, where the catalyst is coordinated *syn* to the substituted double bond.

is *syn* to the coordination site (see complex **27**, Figure 9). However, the second lowest energy TS (**TS11**) is only 0.6 kcal/mol higher in energy, and in this case cycloaddition occurs with the double bond that is *anti* to the site of catalyst coordination. This reaction pathway through the “anti-Corey” coordination mode results in the formation of the opposite enantiomer of the product. The next lowest energy TS involves coordination of the dienophile to the *endo* face of the catalyst (**TS12**, Figure 8). Again, this reaction mode leads to the formation of the minor enantiomer of product.

The large disparity that is seen between the predicted values obtained from theory and the experimental values is likely due to the significant differences between the benzoquinone substrates involved in the calculation and experiment. The computational model used 2-methylbenzoquinone and 1,3-butadiene, whereas the experiment of comparison involved 2-*tert*-butylbenzoquinone and 2-triisopropylsilyloxy-

1,3-butadiene. The steric requirements of both the *tert*-butyl group and the triisopropylsilyloxy group are much larger than the corresponding methyl group and hydrogen atom, which may play a role in selectivity.

For quinone DA reactions, Corey outlined several selection rules for predicting the outcome of a given reaction, based upon detailed studies. Of relevance to this discussion is the following selection rule: “Catalyst coordination at the more basic of the two 1,4-quinone oxygens will predominate, and this mode will lead to the preferred Diels–Alder adduct.”^{3d} For 2-methylbenzoquinone, the most stable Lewis acid complex involves coordination to the less basic lone pair (i.e., complex **28**); however, the second most stable complex (0.04 kcal/mol higher in energy) does involve coordination to the more basic lone pair (i.e., complex **27**). If we follow Corey’s selection rules based on these energies, we would predict that the outcome would be approximately a 50:50 mixture of products arising from the two ground-state complexes. Computationally, the TS that corresponds to the geometry of complex **27** (i.e., **TS10**) is 0.6 kcal/mol more stable than the TS that arises from complex **28** (i.e., **TS11**) (Figure 9). This difference in energy translates to 3 times more product being produced via **TS10** than **TS11**. It appears that 2-methylbenzoquinone is an exception to the selection rule stated above. This is most likely due to the small influence that the Me group has on carbonyl lone pair basicity with respect to the other substituents (including the *t*-Bu group) evaluated by Corey.

Conclusion

In contrast to the limited investigation of Pi and Li, the selectivity of five different classes of dienophiles were evaluated in the chiral, cationic oxazaborolidine-catalyzed Diels–Alder reactions by DFT calculations. Using a model system that closely mirrored the experimental systems, our computational results reinforced the validity of Corey's model in 4 of 5 cases and the experimentally observed enantioselectivity could be reproduced, and in all cases the correct sense of stereoinduction was predicted. In the five classes studied, the minor isomer was formed to a large extent through a pathway that involved coordination of the dienophile to the concave face of the oxazaborolidinium ion catalyst, suggesting that an improvement in selectivity could be achieved through catalyst modifications that disfavor the *endo* mode of coordination.

Acknowledgment. We acknowledge support of this research from the Australian Research Council and the National Institutes of General Medical Sciences, National Institutes of Health (U.S.). Computations were carried out at the Australian Partnership for Advanced Computing (APAC) national facility.

Supporting Information Available: Complete ref 21; Cartesian coordinates for the ground-state reactants, substrate–catalyst complexes, and transition structures; and electronic energies and thermal corrections. This material is available free of charge via the Internet at <http://pubs.acs.org>.

JO802323P